LUNAR HEAT FLOW SIMULATION AND TESTING CHAMBER S.E. Smrekar[1], G. Mungas[1], G. Peters[1], and T.L. Hudson[1], P. Morgan[2], [1]Jet Propulsion Laboratory, California Institute of Technology (Mail Stop 183-501, 4800 Oak Grove Dr., Pasadena CA, 91109; ssmrekar@jpl.nasa.gov), [2] Northern Arizona University (Dept. of Geology, Flagstaff, AZ; paul.morgan@nau.edu).

Introduction: Interior heat flow provides essential constraints on the thermal and chemical evolution of planetary bodies. On the moon, heat flow instrument designs typically have to reach depths below the annual solar thermal wave for the Moon (2-3 m), or alternatively methods must be applied to be able to decouple the influence of the relatively large temperature gradients associated with the annual and diurnal solar thermal wave from the geothermal gradient.

There are many challenges associated with precise heat flow measurements. Key challenges include: 1) accessing the subsurface to sufficient depth in various types of media (e.g. heavily compacted regolith and/or soils with variable in-situ rock distributions), 2) obtaining accurate measurements of the thermal conductivity and thermal gradient in an extremely insolating environment with extremely large surface temperature variations, and 3) calibrating out potential sources of measurement error including a) instrument thermal properties and instrument self-heating, b) local variations in thermal properties generated by the penetration of the instrument, c) thermal conductance of heat through the instrument to the surface, and d) strong potential differences in thermal coupling between the heat flow sensors and the in-situ medium in a vacuum environment associated with partially collapsed borehole walls or intermittent sensor contact with a borehole wall.

To address these issues and provide a testbed for evaluating heat flow measurements and calibration techniques prior to flight, we have constructed a vacuum chamber capable of simulating the lunar heat flow environment.

Lessons from Apollo: Apollo astronauts used hand-operated drills to reach depths of 1.4-2.4 m at Apollo sites 15 and 17. The lunar regolith proved extremely resistant to drilling. As determined from core analyses, the regolith density increases by 90% in the upper 0.2 m (1). Conductivity increases similarly over this interval. Subsequent analysis showed that the lunar regolith is also highly cohesive due to its angular fragment shape from multiple impacts.

Although extremely valuable, the interpretation of the two heat flow measurements from Apollo has been strongly debated. These measurements were done at shallower depths than would be ideal, but the thermal gradient was obtained with reasonable accuracy because they recorded data over several lunar years and appeared to have little conduction of heat down the borehole.

Borehole measurements yielded a heat flow of 21 mW m^{-2} at the *Apollo 15* landing site and 16 mW m^{-2} at the *Apollo 17* landing site [2]. [3] later revised these values downward to 14 to 18 mW m^{-2} based on updated estimates of the thermal conductivity based on propagation of the annual wave. These values are <20% of the Earth's average heat flux of 87 mW m^{-2}. Assuming a steady-state balance between heat flow and heat production, this range of heat flow corresponds to a lunar bulk composition of uranium of 33 to 44 ppb, which is significantly higher than that of Earth's mantle. This discrepancy is difficult to understand in terms of the common origin of Earth and the Moon and fractionation scenarios.

With data from just two sites, heat flow from the Moon is poorly constrained. The International Lunar Network may offer opportunities resolve questions raised by the initial measurements. A number of effects have been proposed to explain the difference in the two measurements. [4] proposed a revised uranium content of 19 ppb for the bulk composition, and an average heat flux of 12 mW m^{-2}. This value is based on models showing that the variable thickness megaregolith acts to insolate the surface, causing a non-steady state heat flux, and causes refraction of the heat flux into areas of higher conductivity. [5] show that the variation in the flux at the two sites can be explained by variable thicknesses of megaregolith containing either a uniform or exponentially decreasing thorium concentration. [6] explain the variation with a model of formation of the Procellarum KREEP Terrane that concentrates radiogenic material in the crust. In this scenario, the compositional differences in the crust account for variations in heat flow. Choice of appropriate landing sites for future missions can readily distinguish between these hypotheses and provide further insight on lunar evolution.

Chamber Description: The chamber consists of a highly insolated 2.5 m high by 1 m diameter cylindrical vacuum chamber filled with simulant (see Figure 1). The axial thermal gradient through the column is controlled by ~isothermal plates at the top and base of the soil column. These plate temperatures are maintained or slowly varied over time by using a cold-biased pumped ice water bath through the plates with active in-line controlled water heaters. Radial heat flow in the soil column is nulled out by active control of the temperature gradient on the cylindrical chamber wall using a passive cold-biased ice-water jacket surrounding a linear array of heater loops distributed down the chamber wall. These heaters are variably controlled to maintain the same axial temperature profile as measured near the center of the soil column with an embedded temperature tether.

In addition to providing a realistic simulated soil temperature profile, the vacuum chamber is required to simulate the low thermal conductivity of lunar regolith that poses a challenge to heat flow measurements. Thermal conductivity is dominated by gas conduction and radiative transfer at low atmospheric pressures or in a vacuum [7-11]. Although we will not be able to achieve lunar pressures in such a large chamber filled with regolith, we will achieve a low enough vacuum (~10 torr) to be in the same thermal regime and achieve the range of thermal conductivities measured by Apollo using variable grainsize regolith. Currently

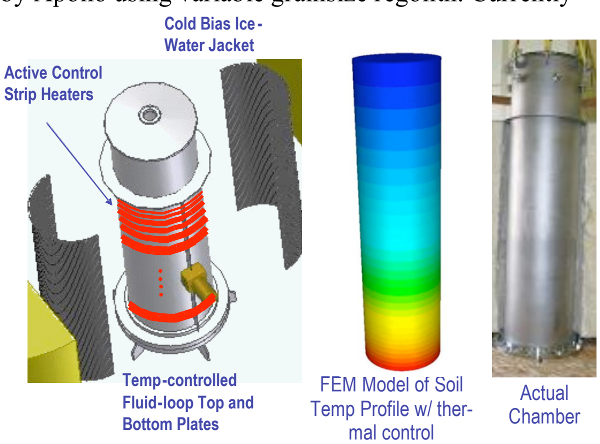

Figure 1. Heat flow test chamber design, thermal model, and actual chamber.

the simulant being used is Mars Mojave Simulant [12]. In the future, more lunar-like materials in terms of particle shape may be used. A uniform initial temperature will be achieved by pumping chilled water along plates at the top and bottom of the chamber, as well as around the chamber walls. A series of heaters on the exterior of the chamber walls will maintain the thermal gradient desired. Thermal conductivity of the simulant is measured independently with several line source devices.

Thermal Modeling. The design of the chamber has been guided by finite element modeling of the chamber. In particular, the insulation, and exterior heater design were validated to ensure that gradients can be maintained in the chamber over long periods (months) and that a transient thermal wave can be applied at the surface without excessive conduction along the walls. All experiments will be validated with this model.

Status and Future Work: By LPSC, we expect to have the chamber filled with regolith and have begun the long process of pumping the chamber down and reaching thermal equilibrium. We will be testing out various designs for temperature sensors, thermal conductivity measurements, and emplacement scenarios. These experiments will be used to optimize the design of a lunar heat flow experiment.

References: [1] Vaniman, D.R. et al. (1991) Lunar Sourcebook, Cambridge Univ. Press. [2] Langseth M.G. et al. (1976) *Proc. Lunar Sci. Conf. 7th,* pp. 3143–3171 [3] Keihm, S. J. and M.G. Langseth (1977) NASA SP-289. [4] Rasmussen, K.L. and P.H. Warren (1985) *Nature, 313*, 121-124. [5] Hagermann, A., and S. Tanaka (2006) *GRL, 33*, doi:10.1029/2006GL027030. [6] Wieczorek, M.A. and R.J. Phillips (2000) *JGR, 105*, 20417-20430. [7-9] Presely M.A. and P.R. Christensen (1997) JGR 102, a: 6535-6549, b: 6551-6566, c: 9221-9229. [10] Presley M.A. and R.A. Craddock (2006) JGR, 111, doi:10.1029/2006JE002706. [11] Huetter, E. S. et al. (2008) JGR 113, doi:10.1029/2008JE003085. [12] Peters, G.H. et al. (2008) *Icarus 197*, 470-479.